



Research Article

Baseline-Free Detection Method for Change of Lateral Stiffness of High-Rise Building Based on Statistical Moment Curvature

Yang Yang ^{1,2}, Zhewei Wang,^{1,2} Bing Xian,^{1,2} Hwa Kian Chai,³ Zhou Yu,⁴ Yao Zhang ⁵, and Tao Zhu^{1,2}

¹School of Civil Engineering, Chongqing University, Chongqing, China

²Institute for Liyang Smart City, Chongqing University, Liyang, China

³School of Engineering, The University of Edinburgh, Edinburgh, UK

⁴MCC Saidi Engineering Technology Co., LTD., Chongqing, China

⁵School of Architecture and Civil Engineering, Xiamen University, Xiamen, China

Correspondence should be addressed to Yang Yang; yangyangcq@cqu.edu.cn and Yao Zhang; zhangyao@xmu.edu.cn

Received 17 January 2023; Revised 28 August 2023; Accepted 20 September 2023; Published 20 October 2023

Academic Editor: Ka-Veng Yuen

Copyright © 2023 Yang Yang et al. This is an open access article distributed under the Creative Commons Attribution License, which permits unrestricted use, distribution, and reproduction in any medium, provided the original work is properly cited.

In recent times, there has been a notable increase in the quantity of high-rise buildings, attributed to the swift advancements in both economic growth and construction technology. Assessing the structural integrity of high-rise buildings is important to ensure their safe operation. However, existing structural health monitoring methods typically require a baseline, involving either the measured dynamic and static responses from an intact structure or the finite element (FE) model corresponding to an undamaged state. These prerequisites are often challenging to acquire in practical scenarios. This study introduces a novel baseline-free method for detecting reduction in the lateral stiffness of high-rise buildings. The method is based on the statistical moment curvature (SMC) concept, determined through applying central difference to the second-order statistical moment of displacement. Initially, theoretical formulas were derived to demonstrate the viability of utilizing SMC for identifying reduction in the lateral stiffness of high-rise buildings. Subsequently, a FE model of a representative high-rise building was constructed to validate the proposed approach and assess its sensitivity, where different structural types and noise levels were considered. Lastly, a field test was conducted on a 33-story shear wall structure to provide additional validation for the proposed method. The results confirmed its effectiveness in accurately detecting reduction in the lateral stiffness of high-rise building. It offers two primary benefits: firstly, it obviates the need for a baseline, rendering it more convenient and applicable in real-world scenarios; secondly, its heightened sensitivity to sudden drops in lateral stiffness allows for early-stage detection of structural damage.

1. Introduction

Structural damage has far-reaching consequences, leading to substantial economic losses as well as posing a significant threat to human life and safety. Structural damage frequently manifests as a reduction in lateral stiffness. Hence, regular inspections and long-term monitoring [1–3] of the high-rise buildings are of paramount importance. Identifying and promptly repairing damages can effectively prevent engineering accidents.

Changes in the structure's modal parameters, such as frequency and mode shape, become inevitable when its lateral stiffness is reduced [4, 5]. Consequently, changes in

dynamic response enable the identification of structural lateral stiffness reduction. In the context of the frequency-based approach, Cawley and Adams [6] were the pioneers in proposing the utilization of a structure's natural frequency for the purpose of damage identification. Subsequent investigations [7–10] revealed that frequency holds the benefits of straightforward measurement and minimal measurement error. However, the natural frequency proves to be insufficiently sensitive to early-stage structural damage, and change in frequency due to damage at distinct locations can be indistinguishable. In comparison to frequency, change in mode shape exhibits higher sensitivity to damage and enable

straightforward localization of the damage. Currently, the popular approaches for damage identification based on mode shapes involve modal assurance criterion (MAC) and cross orthogonality modal assurance criterion (COMAC) [11, 12]. Shahsavari et al. [13] conducted wavelet analysis to detect change in structural vibration modes and used the likelihood ratio test to pinpoint damage in beams. Zhu et al. [14] identified damage in shear buildings using the first-order mode slope and validated the approach through a three-layer test model. Mode shape serves as a good indicator for damage identification. Nonetheless, a considerable discrepancy exists between the actual and theoretical mode shapes of the structure, and acquiring high-order mode shapes poses challenges.

Given that frequency and low-order vibration mode shapes lack sensitivity to damage, while curvature amplifies the influence of damage, the curvature index has emerged as a prominent subject of investigation. Currently, an abundance of literature delves into mode curvature as a damage indicator, and the research in this domain has reached a relatively advanced stage. In detail, Dessi and Camerlengo [15] extensively examined structural damage identification through mode curvature and conducted a comparative analysis of outcomes with damage indices such as frequency and mode shape. Pooya and Massumi [16] introduced a damage identification method that uses the disparity between the genuine damaged structure and the estimated mode curvature as an index. Interestingly, this approach did not necessitate the acquisition of modal parameters from the undamaged structure; nevertheless, the mode curvature accentuated both damage and noise. Cao et al. [17, 18] enhanced the utility of mode curvature in identifying multiple damages while addressing noise interference, achieved by investigating the synergistic potential of wavelet transform and the Teager energy operator. He et al. [19] suggested the averaging of curvature differences across the initial three modes to mitigate the issue of noise-induced local perturbations in the vibration modes. Test and simulation outcomes demonstrated that damage in the composite beam induces an abrupt change in curvature differences, allowing precise detection of the damage's location and severity. Nevertheless, the enhanced modal curvature method continues to exhibit insufficient noise resistance. Typically, the curvature value is approximated using the central difference method. Numerous experts and scholars have undertaken a series of investigations concerning the process of curvature determination. Yang et al. [20] introduced a straightforward Fourier spectrum-based technique for computing beam modal curvature, replacing the conventional central difference method and enhancing the noise resistance in damage identification via modal curvature. Beyond mode curvature, Shi et al. [21] put forth an interpolation approach for computing the lateral displacement envelope curvature of shear-type building structures. The outcomes indicated that the curvature index derived from the interpolation method attains superior accuracy in damage identification compared to the finite difference method. Using the FE

method, Cao et al. [22, 23] demonstrated that the curvature difference of modal flexibility effectively pinpoints damage locations in simply-supported beams, continuous beams, and frame structures. However, they did not account for the impact of noise on the identification accuracy. Consequently, despite the high sensitivity of the curvature index to damage and its precision in identifying structural damage, it remains hindered by the drawback of insufficient noise resistance, posing challenges for its practical application.

Noise has significant influence on the structural response signal, potentially leading to signal distortion in severe instances. Recognizing the present deficiency in noise resistance within various structural damage identification methods, Dinh-Cong et al. [24, 25] introduced a set of damage identification techniques tailored for situations involving incomplete modal data. Zhang et al. [26] introduced damage identification grounded in statistical moment indices. They derived the correlation between the statistical moment index and structural stiffness through a single degree-of-freedom system, confirming its robust noise resistance and significant interest in the topic. Wang et al. [27] employed the fourth strain statistical moment to ascertain the precise location and area of structural damage. Yang et al. [28, 29] suggested identifying structural damage through the fusion of high-order statistical moment indices. The method's efficacy was substantiated by analyzing a range of operational scenarios from a 12-storey standard frame structure shaking table test. Dinh-Cong et al. [30] introduced the manta ray foraging optimization—sequential quadratic programming algorithm—an amalgamation of global and local search techniques designed to attain highly accurate damage identification at minimal computational expense. The aforementioned damage detection techniques all necessitate a precise benchmark model. However, acquiring accurate initial model parameters proves challenging in practical implementations, leading to initial errors within these methodologies.

In this study, the statistical moment theory under the multidegree-of-freedom (MDoF) system was derived. On this basis, the SMC value was approximated by the center difference method, which can identify the reduction of lateral stiffness at a single location and multiple locations, and the reduction of lateral stiffness at different levels. In addition, the influence of different structural forms, external excitation, and environmental noise level in the proposed method was also investigated. The proposed method has also been validated by both numerical simulation of a centralized mass model of cantilever structure and field measurement of a 33-storey shear wall structure.

2. Theory of Statistical Moments

2.1. Theoretical Analysis of Single Degree-of-Freedom (SDoF) Statistical Moments. The motion equation of a single degree-of-freedom linear elastic structure can be expressed as follows:

$$m\ddot{x}(t) + c\dot{x}(t) + kx(t) = -m\ddot{x}_g(t), \quad (1)$$

where m , c , and k are the mass, damping, and stiffness of the structure, respectively; $x(t)$, $\dot{x}(t)$, and $\ddot{x}(t)$ are the displacement, velocity, and acceleration responses, respectively; and $\ddot{x}_g(t)$ is acceleration of ground excitation. Once the displacement is measured, the second-order statistical moment can be obtained as follows:

$$M_d^2 = \frac{1}{N_s} \sum_{i=1}^{N_s} (x_i - \bar{x}_i)^2, \quad (2)$$

where x_i is the i th data in the displacement time history, \bar{x}_i is the corresponding mean, and N_s is the total number of data. It can be derived that the second-order statistical moment of displacement (equation (2)) is a dynamic characteristic which is directly related to mass and stiffness. In fact, equation (1) can be simplified as follows:

$$\ddot{x}(t) + 2\omega_0\xi\dot{x}(t) + x(t) = -\ddot{x}_g(t), \quad (3)$$

where ξ and ω_0 are structure damping ratio and circular natural frequency, respectively. For linear elastic structure, the variance of structural response σ^2 can be expressed as follows:

$$\sigma^2 = \int_{-\infty}^{+\infty} |H(\omega)|^2 S_f(\omega) d\omega, \quad (4)$$

where $S_f(\omega)$ is the power spectral density function of ground excitation. When the ground excitation is ideal white noise, $S_f(\omega)$ can be regarded as a constant S_0 in frequency domain and $H(\omega)$ is the frequency response function of a structure that can be expressed as follows:

$$H(\omega) = \frac{1}{m\sqrt{(\omega_0^2 - \omega^2)^2 - (2\xi\omega_0\omega)^2}}. \quad (5)$$

Based on the derivation and conclusion in [26, 27], the second-order statistical response of displacement is just equivalent to the variance of displacement; therefore, one can easily obtain the following equation:

$$M_d^2 = \sigma^2 = \int_{-\infty}^{+\infty} |H(\omega)|^2 S_f(\omega) d\omega = \frac{\pi S_0}{2\xi\sqrt{mk^3}}. \quad (6)$$

It can be seen from equation (6) that the change of structural stiffness will inevitably lead to the change of statistical moment of structural response, so the statistical moment can be considered as the structural damage identification index.

2.2. Theoretical Analysis of Statistical Moment with Multi-degree-of-Freedom (MDOF). For linear multidegree-of-freedom systems with viscous damping, as shown in Figure 1, K_i is the stiffness of the i th element and M_i is the mass at the i th node. The dynamic equations of motion can be written as follows:

$$\mathbf{M}\ddot{\mathbf{x}}(t) + \mathbf{C}\dot{\mathbf{x}}(t) + \mathbf{K}\mathbf{x}(t) = \mathbf{P}(t), \quad (7)$$

where \mathbf{M} , \mathbf{C} , and \mathbf{K} are the mass, damping, and stiffness matrix, respectively; $\ddot{\mathbf{x}}(t)$, $\dot{\mathbf{x}}(t)$, and $\mathbf{x}(t)$ are the acceleration, velocity, and displacement vector, respectively; and $\mathbf{P}(t)$ is the excitation vector. For the i th node, once the displacement time history is measured, the second-order statistical moment can be obtained as follows:

$$M_{d,i}^2 = \frac{1}{N_s} \sum_{j=1}^{N_s} (x_{j,i} - \bar{x}_{j,i})^2, \quad (8)$$

where, $x_{j,i}$ is the j th data in the displacement time history, $\bar{x}_{j,i}$ is the corresponding mean, and N_s is the total number of data. Similar to the MDOF system, it can also be derived that the second-order statistical moment of displacement (equation (8)) is a dynamic characteristic which is directly related to mass and stiffness matrix. In fact, by using the superposition method, equation (7) can be simplified as follows:

$$\ddot{Y}_n(t) + 2\xi_n\omega_n\dot{Y}_n(t) + \omega_n^2 Y_n(t) = \frac{P_n(t)}{M_n}, \quad n = 1, 2, \dots, N, \quad (9)$$

where M_n , N , ξ_n , and ω_n are the n th generalized mass, mode number, modal damping ratio, and circular natural frequency, respectively; $P_n(t)$ is n th generalized force; and $Y_n(t)$ is the n th mode corresponding generalized coordinates that can be expressed as follows:

$$Y_n(t) = \int_0^t P_n(\tau) h_n(t - \tau) d\tau, \quad (10)$$

$$h_n(t) = \frac{1}{M_n\omega_{Dn}} \exp[-\xi_n\omega_n(t - \tau)] \sin \omega_{Dn}t, \quad (11)$$

$$\omega_{Dn} = \omega_n(1 - \xi_n^2)^{1/2}.$$

The relative displacement response of the i th node can be expressed as the linear superposition of several vibration modes, namely,

$$d_i(t) = \sum_{n=1}^N B_n Y_n(t) = \sum_{n=1}^N (\varphi_n^i - \varphi_n^{i-1}) Y_n(t). \quad (12)$$

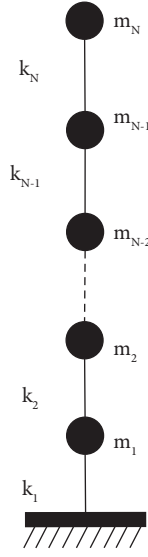


FIGURE 1: A typical MDoF structure.

Under the condition of stationary excitation, the response process will also be a stationary distribution. Combined with equations (10)–(12), the autocorrelation function can be expressed as follows:

$$R_{di}(\tau) = E[d_i(t)d_i(t+\tau)] = E\left[\sum_{m=1}^N \sum_{n=1}^N B_m B_n Y_m(t) Y_n(t+\tau)\right] \quad (13)$$

$$= \sum_{m=1}^N \sum_{n=1}^N \int_0^\infty \int_0^\infty B_m B_n R_{P_m P_n}(\theta_2 - \theta_1) h_m(t - \theta_1) h_n(t + \tau - \theta_2) d\theta_1 d\theta_2,$$

where θ_1 , θ_2 , and τ are imaginary time variables and $R_{P_m P_n}(\tau)$ is the covariance function of $P_m(t)$ and $P_n(\tau+t)$. Through variable substitution, the autocorrelation function

of relative displacement response can be expressed as follows:

$$u_1 = t - \theta_1, u_2 = t + \tau - \theta_2, du_1 = -d\theta_1, du_2 = -d\theta_2, \quad (14)$$

$$R_{di}(\tau) = \sum_{m=1}^N \sum_{n=1}^N \int_0^\infty \int_0^\infty B_m B_n R_{P_m P_n}(\tau - u_2 + u_1) h_m(u_1) h_n(u_2) du_1 du_2. \quad (15)$$

The power spectral density function can be obtained by Fourier transform of the autocorrelation function of the relative displacement response as follows:

$$S_{di}(\omega) = \frac{1}{2\pi} \int_{-\infty}^{+\infty} R_{di}(\tau) \exp(-i\omega\tau) d\tau. \quad (16)$$

Substituting equation (15) into equation (16), the autocorrelation function of the relative displacement response can be expressed as follows:

$$S_{di}(\omega) = \sum_{m=1}^N \sum_{n=1}^N B_m B_n H_m(-i\omega) H_n(i\omega) S_{P_m P_n}(\omega), \quad (17)$$

where $S_{P_m P_n}(\omega)$ is the cross-power spectral density function of $P_m(t)$ and $P_n(t)$, and

$$H_m(-i\omega) = \frac{1}{K_m [1 - 2i\xi_m(\omega/\omega_m) - (\omega/\omega_m)^2]}, \quad (18)$$

$$H_n(i\omega) = \frac{1}{K_n [1 - 2i\xi_n(\omega/\omega_n) - (\omega/\omega_n)^2]},$$

where K_m and K_n are the m th and n th generalized stiffness, respectively. For the small damping system, the cross term in equation (17) has limited contribution to the structural response, so equation (17) can be simplified as follows:

$$S_{di}(\omega) = \sum_{n=1}^N B_n^2 |H_n(i\omega)|^2 S_{P_n P_n}(\omega). \quad (19)$$

When the base excitation follows a Gaussian distribution of zero mean value, the power spectral density function is a constant S_0 , and the cross-power spectral density function $S_{P_n P_n}(\omega)$ of external load $P_n(t)$ can be expressed as follows:

$$S_{P_n P_n}(\omega) = \Phi_n^T \mathbf{M} \mathbf{I} \mathbf{I}^T \mathbf{M}^T \Phi_n S_0, \quad (20)$$

where \mathbf{I} is a column vector with all elements of 1 and Φ_n is the n th mode shape vector. From the relationship between the power spectral density function and variance, it can be obtained that the second-order central moment of the relative displacement response of the i th node is as follows:

$$\sigma_{d,i}^2 = \int_{-\infty}^{+\infty} S_{di}(\omega) d\omega = \frac{\pi}{2} \sum_{n=1}^N \frac{\Phi_n^T \mathbf{M} \mathbf{I} \mathbf{I}^T \mathbf{M}^T \Phi_n S_0}{M_n^2 \omega_n^3 \xi_n} (\phi_n^i - \phi_n^{i-1})^2, \quad (21)$$

where ϕ_n^i and ϕ_n^{i-1} are the values of n th mode shape at the i th node and the $(i-1)$ th node.

On the one hand, the second-order statistical response of displacement is just equivalent to the variance of displacement; similarly [26, 27], on the other hand, higher-order modes only contain a very small portion of energy so that the fundamental mode itself is enough for vibration analysis. Therefore, equation (21) can be rewritten as follows:

$$M_{d,i}^2 = \sigma_{d,i}^2 = \frac{\pi}{2} \frac{\Phi_1^T \mathbf{M} \mathbf{I} \mathbf{I}^T \mathbf{M}^T \Phi_1 S_0}{M_1^2 \omega_1^3 \xi_1} (\phi_1^i - \phi_1^{i-1})^2. \quad (22)$$

Within the realm of damage identification research, the common assumption involves the preservation of mass while investigating alterations in stiffness to determine structural damage. Equation (22) readily illustrates that, with mass held constant, any alteration in stiffness due to damage will manifest as shifts in the measured frequency and vibration mode values. This observation underscores the continued utility of the statistical moment in identifying structural damage within an MDoF system. Under the assumption of equidistant measuring points, the SMC index, as introduced in this study, is derived via central difference approximation using the second-order statistical moment of relative displacement as follows:

$$\text{SMC}_i = \frac{M_{d,i+1}^2 - 2M_{d,i}^2 + M_{d,i-1}^2}{h^2}, \quad (23)$$

where h is the distance between neighboring nodes. When the spacing of neighboring nodes is nonuniform, for example, the spacing between the i th and the $(i-1)$ th nodes is h_i and the spacing between the i th and the $(i+1)$ th nodes is h_{i+1} , the SMC can be obtained as follows:

$$\text{SMC}_i = \frac{2(h_i M_{d,i+1}^2 - (h_i + h_{i+1}) M_{d,i}^2 + h_{i+1} M_{d,i-1}^2)}{h_i h_{i+1} + h_i^2 h_{i+1}}. \quad (24)$$

Through the derivation of the above formula, the second-order SMC of displacement is used as the damage index to identify the damage of the high-rise building structure. It should be noted that the time history of displacement at the $(i-1)$ th, i th, and $(i+1)$ th node is required to obtain the corresponding SMC at the i th node of a high-rise building. Hence, to evaluate the damage which may occur at any node, it is recommended that the responses at all nodes are measured. The specific steps are shown in Figure 2.

- (1) Obtain the displacement time-history response of the nodes in the same vertical plane in the same horizontal direction of the high-rise building structure.
- (2) Analyze the displacement signal, obtain the lowest natural frequency of the structure, extract displacement signal of each node under the lowest natural frequency, calculate the second-order statistical moment of the relative displacement of each node, and solve the SMC value of the corresponding node.
- (3) Draw the curve with the height of each node and the SMC value of the corresponding node, observe the sudden change of the curve, and identify the sudden change position of lateral stiffness.
- (4) When structure displacement response signal is contaminated by noise, a small sudden change will result in judgment of SMC curve. In order to get the damage position clearly and visually, the box plot [31, 32] is used to determine the upper and lower limit of the curve. Exceeding the limit is regarded as sudden change, and the corresponding node can be regarded as the location of damage. The box plot gets the upper (UL) and lower limits (LL) as follows:

$$\begin{aligned} \text{UL} &= Q_3 + 1.5 \times (Q_3 - Q_1), \\ \text{LL} &= Q_1 - 1.5 \times (Q_3 - Q_1), \end{aligned} \quad (25)$$

where Q_1 is the first quartile and Q_3 is the third quartile.

3. Numerical Simulation

3.1. Model Introduction. A FE model of a 33-story high-rise building has been constructed according to [28, 29] as shown in Figure 3. The initial modulus of elasticity of the column is $E_0 = 7.751 \times 10^9$ N/m², the height of each layer is $h = 0.3$ m, the line density is $m_C = 7.35$ kg/m, the beam is considered as a rigid body, the span $l = 0.6$ m, the mass $m_b = 26.35$ kg, and the damping ratio $\xi_i = 0.05$ ($i = 1, 2$). The damping type used in this model is Rayleigh damping. The time history of dynamic response of the structure subjected to prescribed excitation can be obtained by the Newmark- β method. Eight cases have been considered in this study, as shown in Table 1.

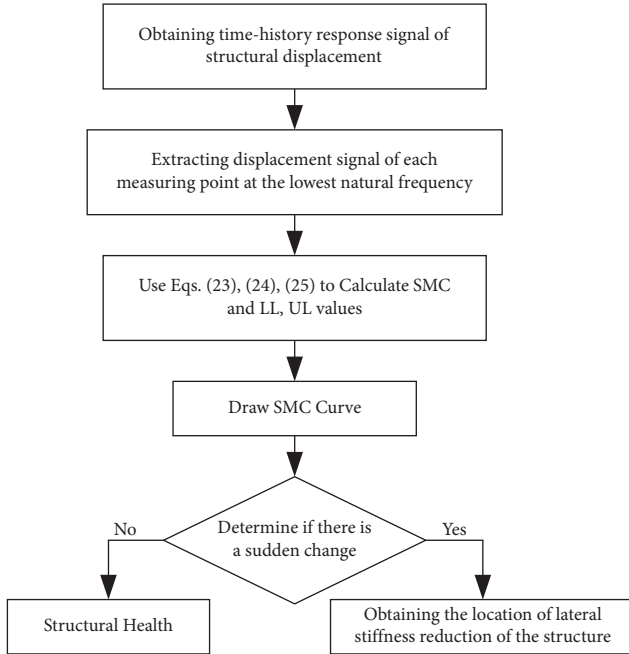


FIGURE 2: The flowchart for structural damage identification.

The reduction of the lateral stiffness of the element indicates that the floor and column of this floor may be damaged.

3.2. Numerical Validation. To ascertain the viability of the proposed method, its effectiveness has been evaluated across varying conditions of environmental noise, external excitation, and different structural forms. The ambient noise was simulated by white noise, and the signal-to-noise ratio (SNR) can be defined as follows:

$$\text{SNR} = 10 \times \log \left(\frac{1/N \sum_{i=1}^N y_i^2}{1/N \sum_{i=1}^N \sigma_i^2} \right), \quad (26)$$

where N is the number of data, y_i is the signal with noise at the i th moment, and σ_i is the noise value at the i th moment. Concurrently, due to the diversity of actual structures, structural models with constant stiffness, gradual stiffness change, and stage stiffness change were simulated by changing the elastic modulus of the column. Additionally, given the prevalent nonstationary characteristics of stochastic dynamic loads in practical engineering scenarios, simulations incorporate Gaussian white noise, El-Centro wave, and Kobe wave as external excitations. In summary, the simulated operating conditions are shown in Table 2.

3.2.1. Constant Stiffness Structure. With Gaussian white noise applied as external excitation, the SMC curve was utilized to determine the location of sudden lateral stiffness changes. The outcomes of Case 1 to Case 5 are presented in Figure 4. Generally, the proposed method can identify the damages accurately for all the 5 cases, regardless of the noise level. For Case 1, the SMC curve demonstrates an ideally flat profile, indicating there is no damaged story. For Case 2, where the 15th story was

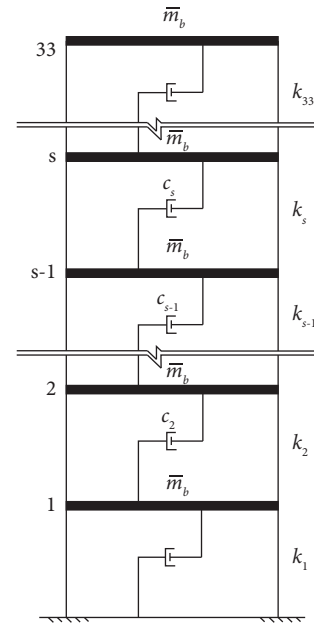


FIGURE 3: Plane model of high-rise structure.

TABLE 1: Details of damage cases.

Case	Damage location	Node number	Stiffness reduction
1	—	—	—
2	Element 15	14-15	5%
3	Element 4, 23	14-15	10%
4	Element 18, 19	17-19	15%
5	Element 14, 15, 16	13-16	20%
6	Element 5	4-5	20%
7	Element 6	5-6	10%
8	Element 5, 6	4-6	20%

damaged, the SMC curve changed abruptly beyond the lower limits at the damaged story while the SMC curve changed abruptly beyond the upper limits at the 14th and 16th stories. This is because the statistical moment value increases at the 15th story due to the reduction of lateral stiffness, and the statistical moment values at the 13th, 14th, 16th, and 17th stories remains the same because these stories are not damaged; hence, the SMC value at the 15th story decreases, and the SMC values at the 14th and 16th stories increase according to equation (23). For Case 3, where there are two separate damages at the 4th and 23rd stories, it also exhibits abrupt deviations that surpass the upper and lower limits. For Case 4 and Case 5, where there are two and three adjoining stories damaged at the same time, similar observations can be obtained. It is noteworthy that for Case 5, the SMC value at the 15th story returns near to zero because the statistical moment values at the 14th, 15th, and 16th story increase simultaneously. Figure 5 shows the identification results when the El-Centro wave was used as external excitation. It can be observed that even if the external excitation changes, the proposed method can still identify all the damages successfully.

TABLE 2: List of numerical simulation cases.

Structural form	External excitation	Cases	Noise conditions
Constant stiffness structure	Gaussian white noise	Cases 1–5	Noise-free SNR = 40 dB SNR = 30 dB
	El-Centro wave	Cases 1–5	Noise-free SNR = 40 dB SNR = 30 dB
Gradual stiffness structure	Gaussian white noise	Cases 1–5	Noise-free SNR = 40 dB SNR = 30 dB
	Kobe wave	Cases 1–5	Noise-free SNR = 40 dB SNR = 30 dB
Structures with stage-change stiffness	Gaussian white noise	Cases 1, 2, and 6–8	Noise-free SNR = 40 dB SNR = 30 dB
	Kobe wave	Cases 1, 2, and 6–8	Noise-free SNR = 40 dB SNR = 30 dB

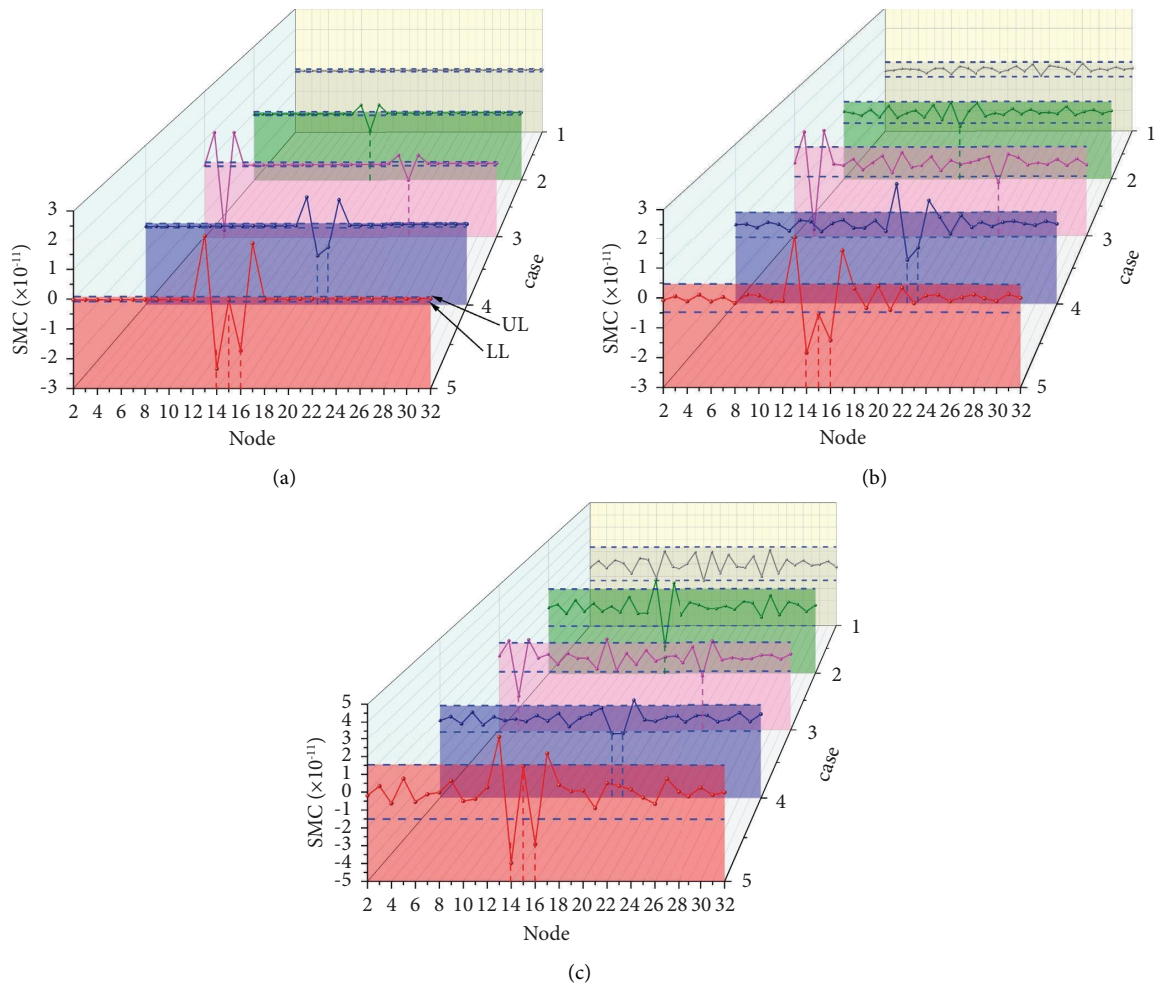


FIGURE 4: Identification results of constant stiffness structures under Gaussian white noise excitation: (a) noise-free; (b) SNR = 40 dB; (c) SNR = 30 dB.

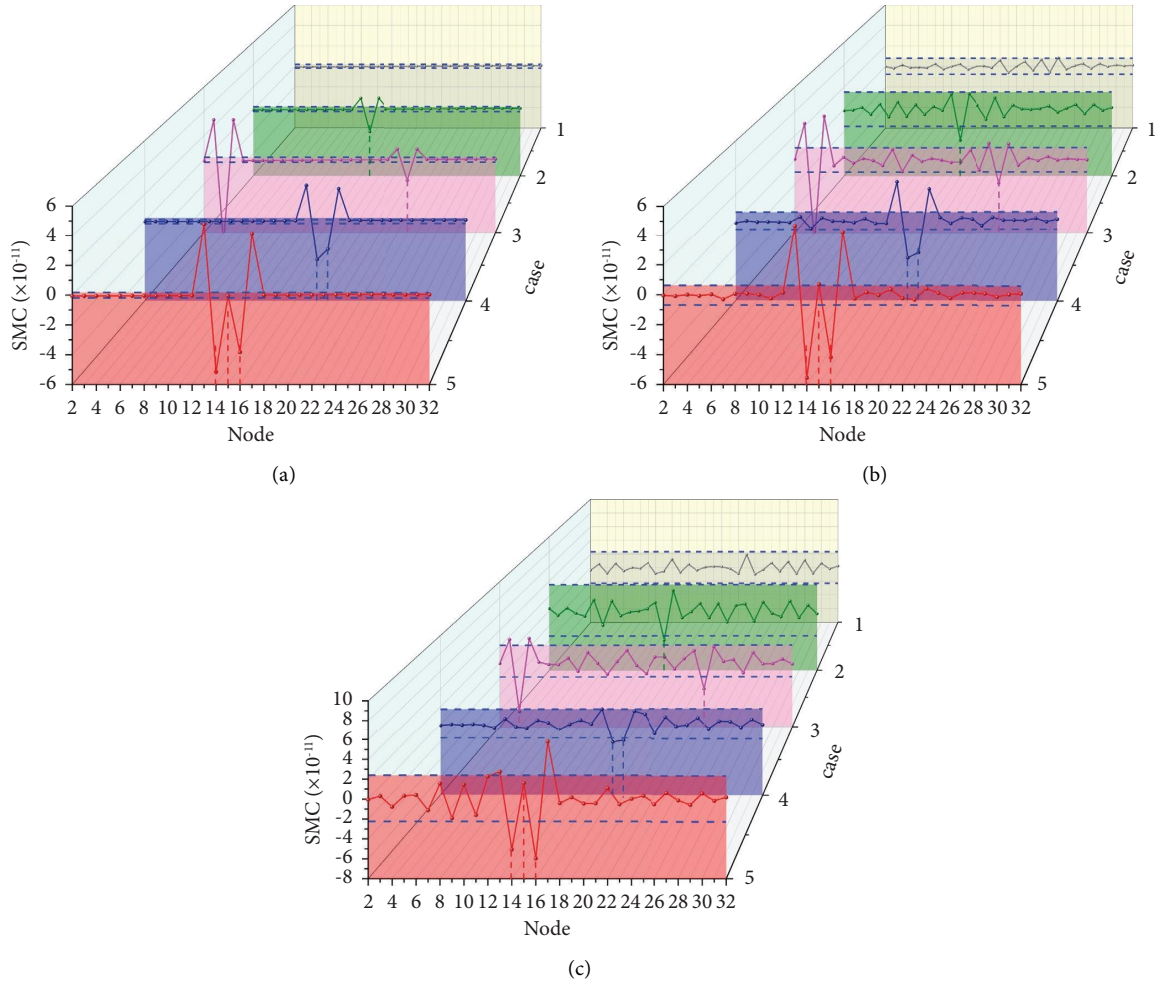


FIGURE 5: Identification results of constant stiffness structures under El-Centro wave excitation: (a) noise-free; (b) SNR = 40 dB; (c) SNR = 30 dB.

3.2.2. Gradual Stiffness Structure. The elastic modulus of the column in the numerical model of gradual stiffness structure was changed to $E_0 = (1 - 0.01 \times n) \times 7.751 \times 10^9 \text{ N/m}^2$ ($n = 1, 2, \dots, 33$) to simulate the gradual stiffness structure. Similarly, Gaussian white noise and Kobe wave were used as external excitations for the simulation calculation. The results are shown in Figures 6 and 7.

For stiffness gradient structures (shown in Figures 6 and 7), whether Gaussian white noise or Kobe wave was used as base excitation, SMC can effectively identify the location under the preset working conditions (Cases 1–5). At the same time, considering the influence of different noise levels, the identification results are still accurate when SNR = 40 dB and 30 dB, without misjudgment. Therefore, the proposed method in this study is still applicable to gradual stiffness structures.

3.2.3. Stiffness Stage Changing Structure. The bottom layer of the actual high-rise building structure often has special purposes, resulting in a large difference between the lateral stiffness of the bottom layer and the upper layers. Therefore, there should be a sudden change in stiffness for this type of

structure. The elastic modulus of the numerical model column was changed to $E_i = 1.3 \times 7.751 \times 10^9 \text{ N/m}^2$, $h_i = 0.5 \text{ m}$ ($i = 1, 2, \dots, 5$) and $E_i = 7.751 \times 10^9 \text{ N/m}^2$, $h_i = 0.3 \text{ m}$ ($i = 6, 7, \dots, 33$). Case 1, Case 2, and Cases 6–8 are considered herein, and Gaussian white noise and Kobe wave were used as external excitations. The identification results are shown in Figures 8 and 9. It can be seen that the proposed method can identify the sudden change in stiffness at the 6th story for all the cases regardless of the type of external excitation. Comparing Case 1 and Case 6, the SMC indicator at the 6th story is less obvious because the stiffness reduction at element 5 makes the stiffness stage-change smoother. However, comparing Case 1 and Case 7, the SMC indicator at the 6th story is more obvious because the stiffness reduction at element 6 makes the stiffness stage change sharper. Similar trend can be seen in Case 8.

3.3. Comparative Analysis of Model-Free Detection Methods. This study also compared the effectiveness of the proposed method with the modal curvature difference method [16] and the flexibility curvature difference method [19]. A comparative analysis scenario involving a 20% reduction

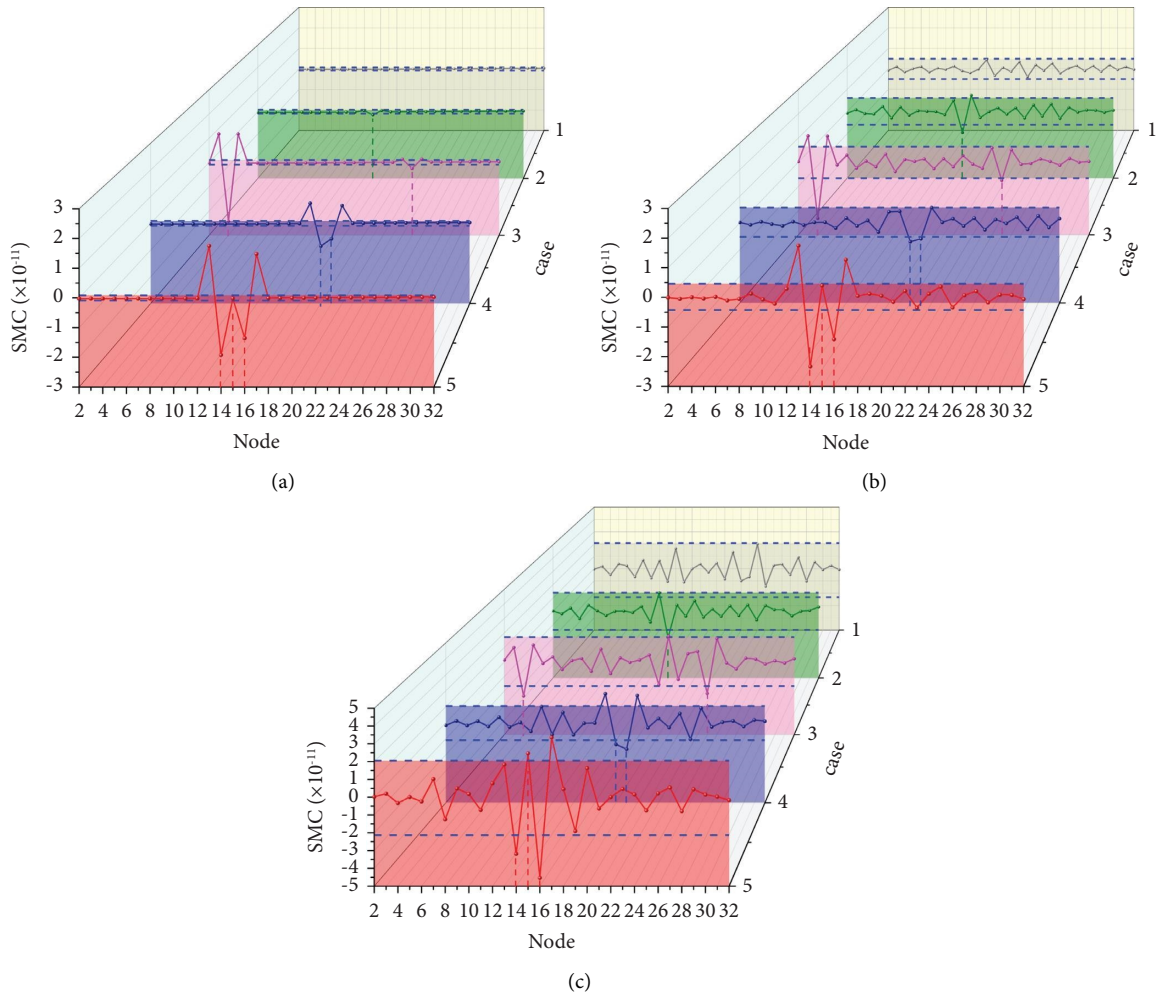


FIGURE 6: Identification results of gradual stiffness structures under Gaussian white noise excitation: (a) noise-free; (b) SNR = 40 dB; (c) SNR = 30 dB.

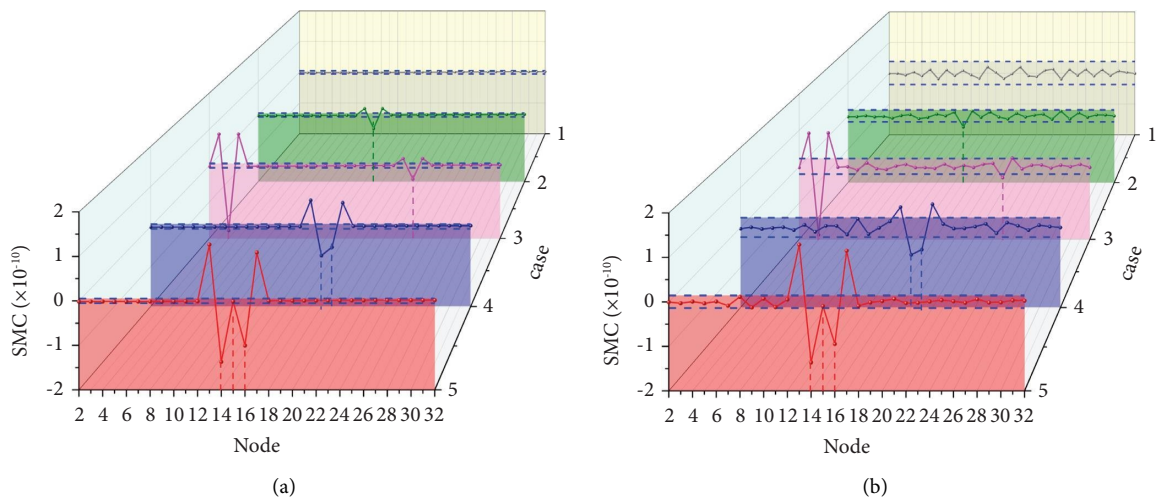


FIGURE 7: Continued.

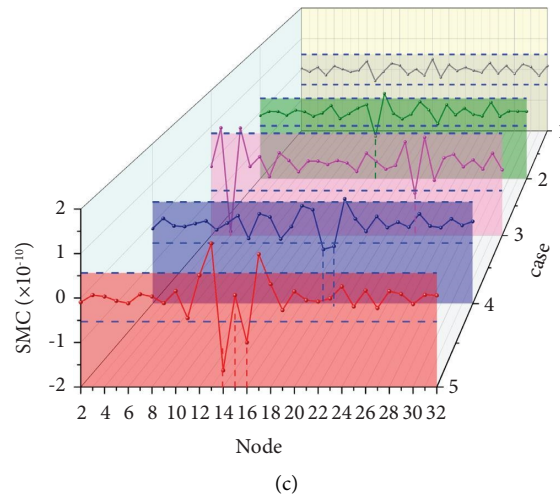


FIGURE 7: Identification results of gradual stiffness structures under Kobe wave excitation: (a) noise-free; (b) SNR = 40 dB; (c) SNR = 30 dB.

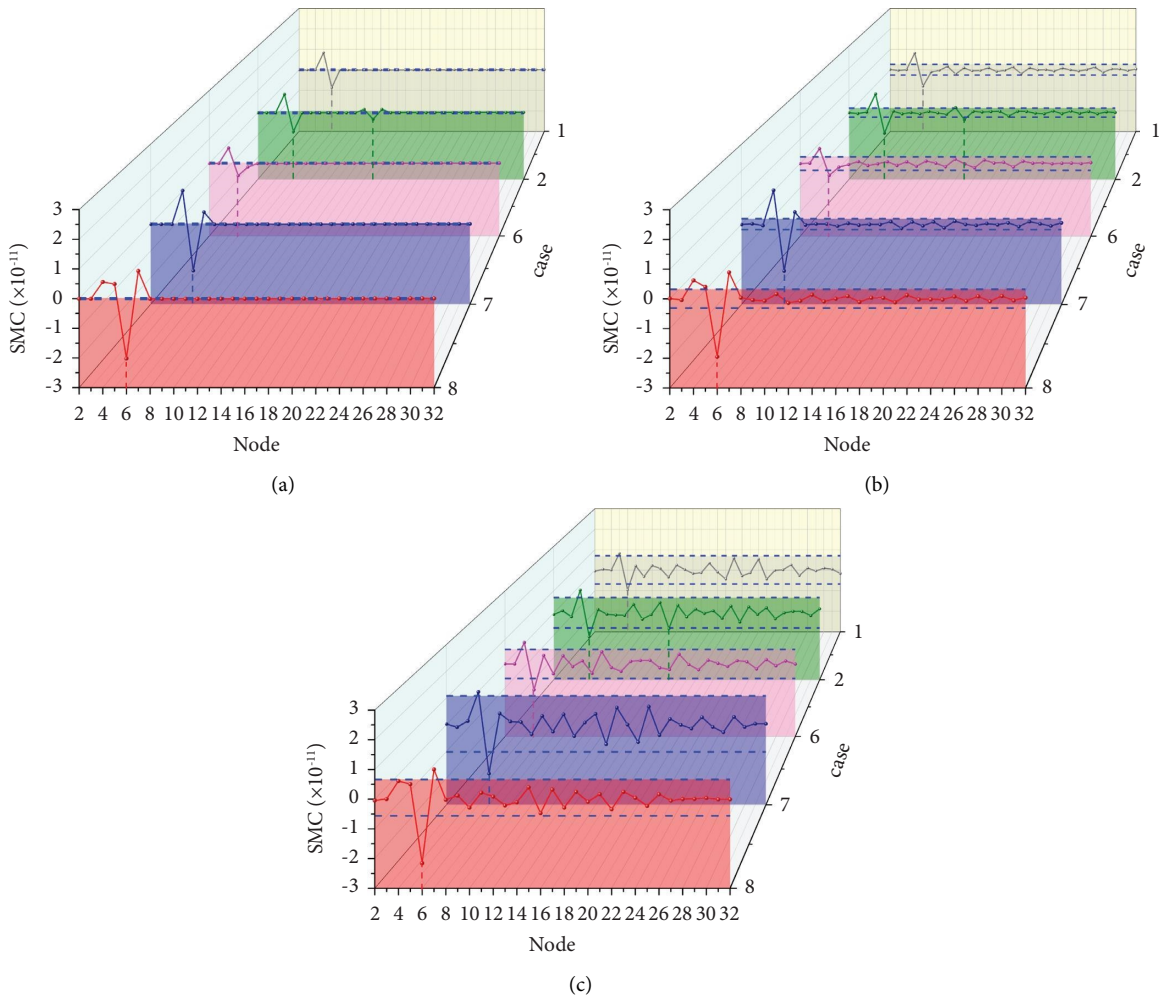


FIGURE 8: Identification results of stiffness stage-changing structure under Gaussian white noise excitation: (a) noise-free; (b) SNR = 40 dB; (c) SNR = 30 dB.

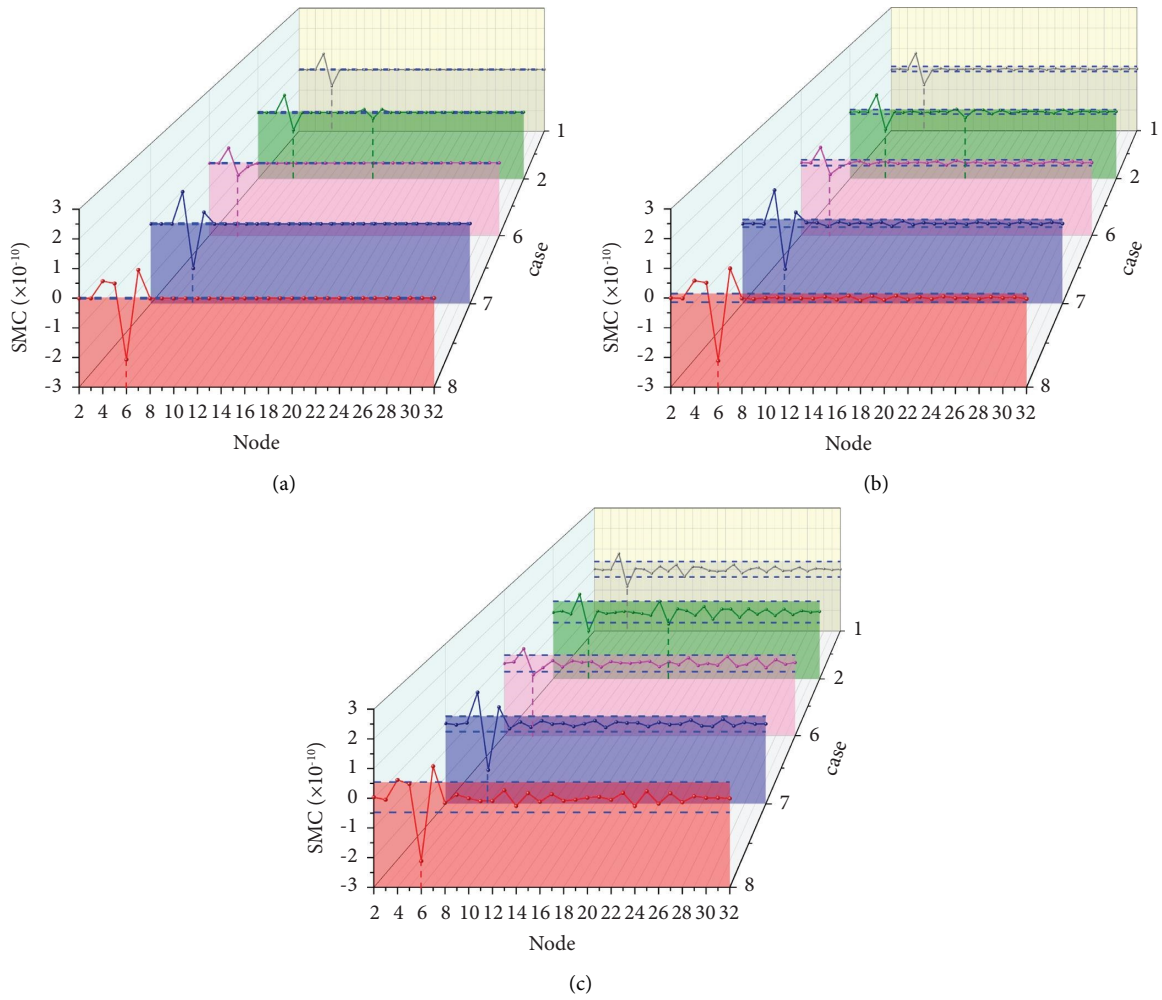


FIGURE 9: Identification results of stiffness stage changing structure under Kobe wave excitation: (a) noise-free; (b) SNR = 40 dB; (c) SNR = 30 dB.

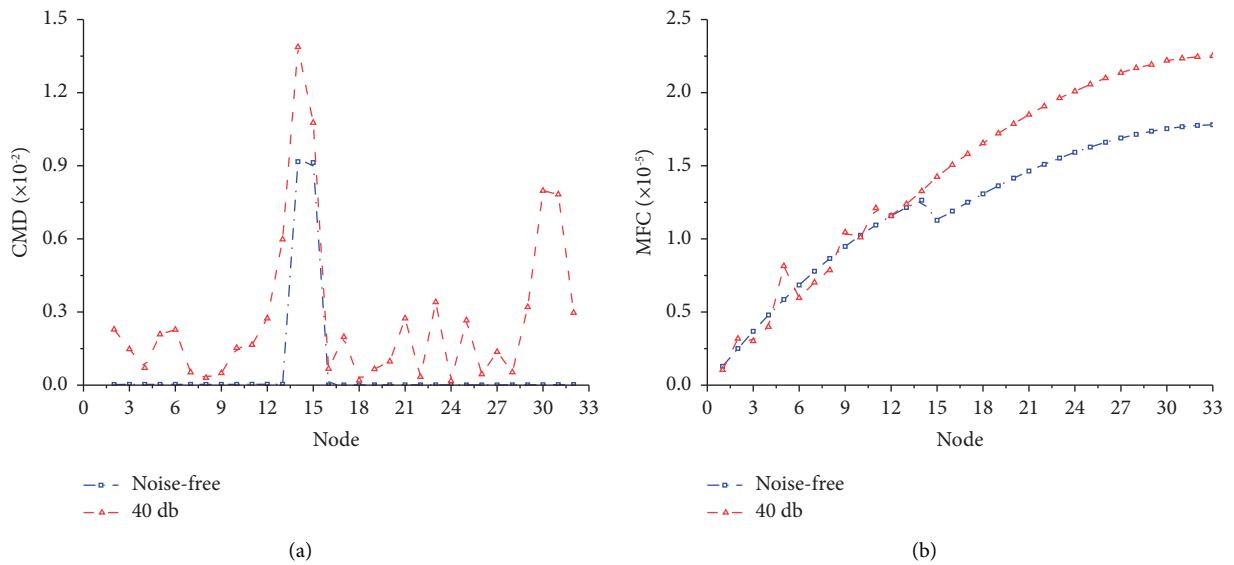


FIGURE 10: Continued.

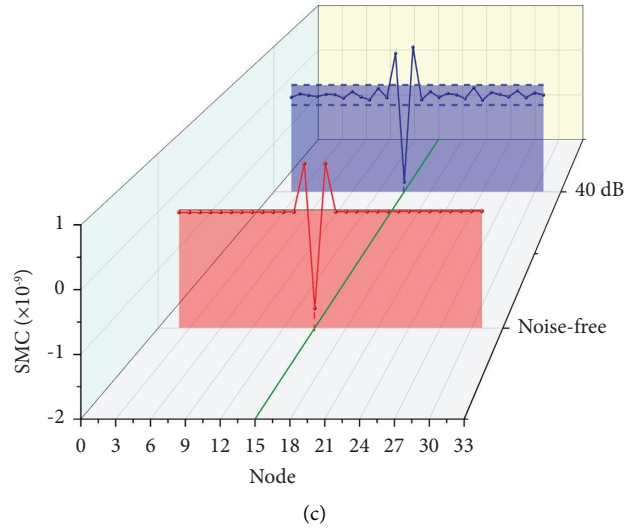


FIGURE 10: Comparison and analysis diagram of recognition results of different detection methods: (a) modal curvature difference method; (b) flexibility curvature difference method; (c) proposed method.

TABLE 3: Comparison and analysis of recognition results of different detection methods.

Method	Whether the stiffness reduction position can be judged	Is it easy to misjudge	Whether to refer to the initial state data of the structure	The sensitivity coefficients
Modal curvature difference method	Yes	Yes	Yes	7.12
Flexibility curvature difference method	Yes	Yes	Yes	7.75
Proposed method	Yes	No	No	579.36

TABLE 4: Properties of the high-rise building.

Component	Floor	Elevation	Strength grade
Beam, plate	All floors	—	C30
	1~9	Base top~11.150	C50
Column, shear wall	10~15	11.150~27.950	C45
	16~19	27.950~39.150	C40
	20~24	39.150~53.150	C35
	25~33	53.150~78.350	C30

in lateral stiffness at the 15th story under noise-free and 40 dB conditions was conducted. The identification results are shown in Figure 10.

Table 3 shows the comparative assessment of the effectiveness. The proposed method can obtain the identification results by only considering the measurement data, without comparing the data before and after the structure is damaged. It uses the time history of displacement directly and does not need to extract the modal parameters, so it has stronger engineering applicability. Moreover, sensitivity analysis of indicators [33] shows that the proposed method exhibits higher sensitivity to changes in stiffness.

4. Field Measurement

In order to verify the applicability of the proposed method, a new high-rise building in Chongqing was tested, the upper residential units and lower garage of which have obvious stiffness change. The structure has a total of 33 floors, the lower 1 to 5 floors are garages, and the upper 6 to 33 floors are residential units. The total height of the structure is about 102.1 m: the floor height of garage is 4.5 m and the height of residential units is 2.8 m. Table 4 shows the properties of the high-rise building and Figure 11 shows its picture and front and side elevations.

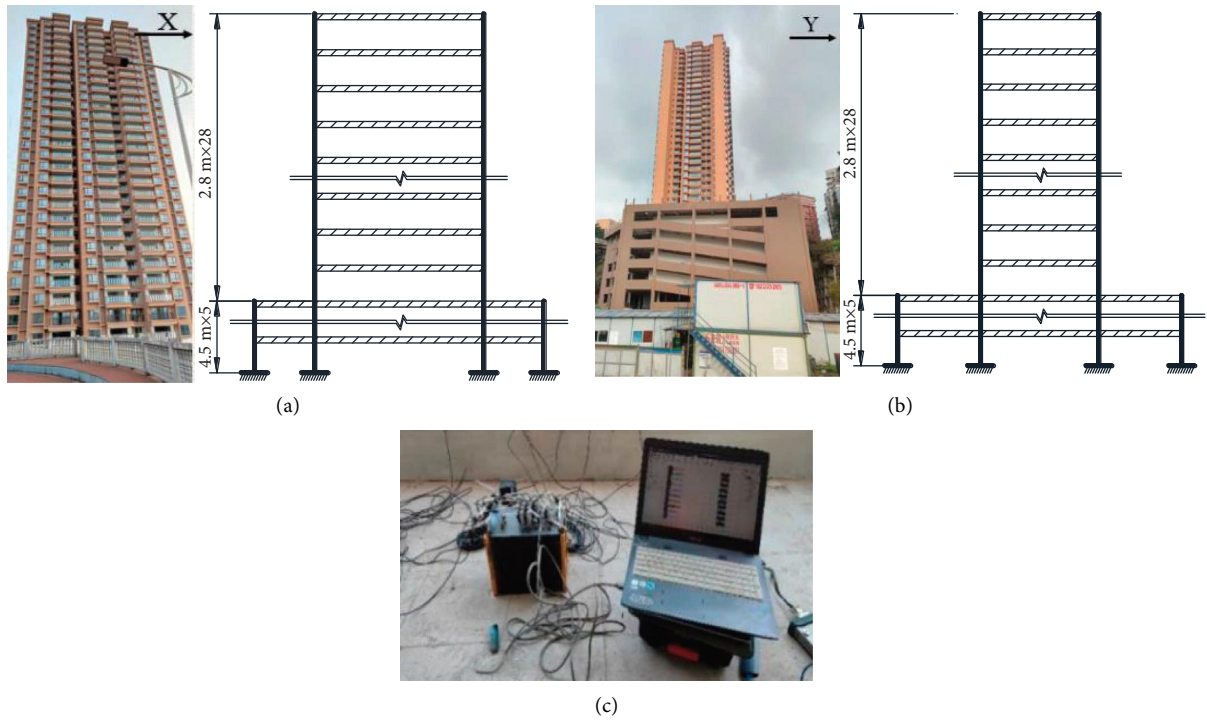


FIGURE 11: Photograph of high-rise building and test equipment: (a) front elevation; (b) side elevation; (c) test equipment.

Based on the design drawing, the centroid of each floor was inferred to be located around the stairwell. Ten horizontal acceleration sensors (Model: 2D001H) were uniformly positioned adjacent to each stairwell. The data acquisition instrument (Model: DH5902) along with a supporting laptop (depicted in Figure 11(c)) was placed on the intermediate floor of each group. Limited by the number of sensors, the field test was divided into five groups to measure the entire building: 1–9 floors, 5–14 floors, 12–21 floors, 19–28 floors, and 24–32 floors, respectively. There were three floors or more between every two groups for repeated measurement. Each group measured the acceleration response in X and Y directions. X and Y represent the length and width of the structural plane, respectively. The sampling duration was 50 s, and the sampling frequency was 100 Hz.

The selected accelerations and the corresponding spectrum can be seen in Figures 12 and 13. The spectral analysis reveals the lowest natural frequency in the X direction to be 0.891 Hz and in the Y direction to be 0.818 Hz. Integrating the measured acceleration yields the displacement response of the structure, and the approach presented in this study was applied to identify the abrupt change in lateral stiffness position. In Figure 14, the SMC curve shows an abrupt change at the 6th floor. This observation confirms the presence of stiffness change. This aligns with the structural design specifications: floors 1–5 have a plane area of 2540.86 m^2 , 86 columns, and around 160 shear walls, whereas floors 6–33 have a plane area of 627.72 m^2 , 4 columns, and about 140 shear walls.

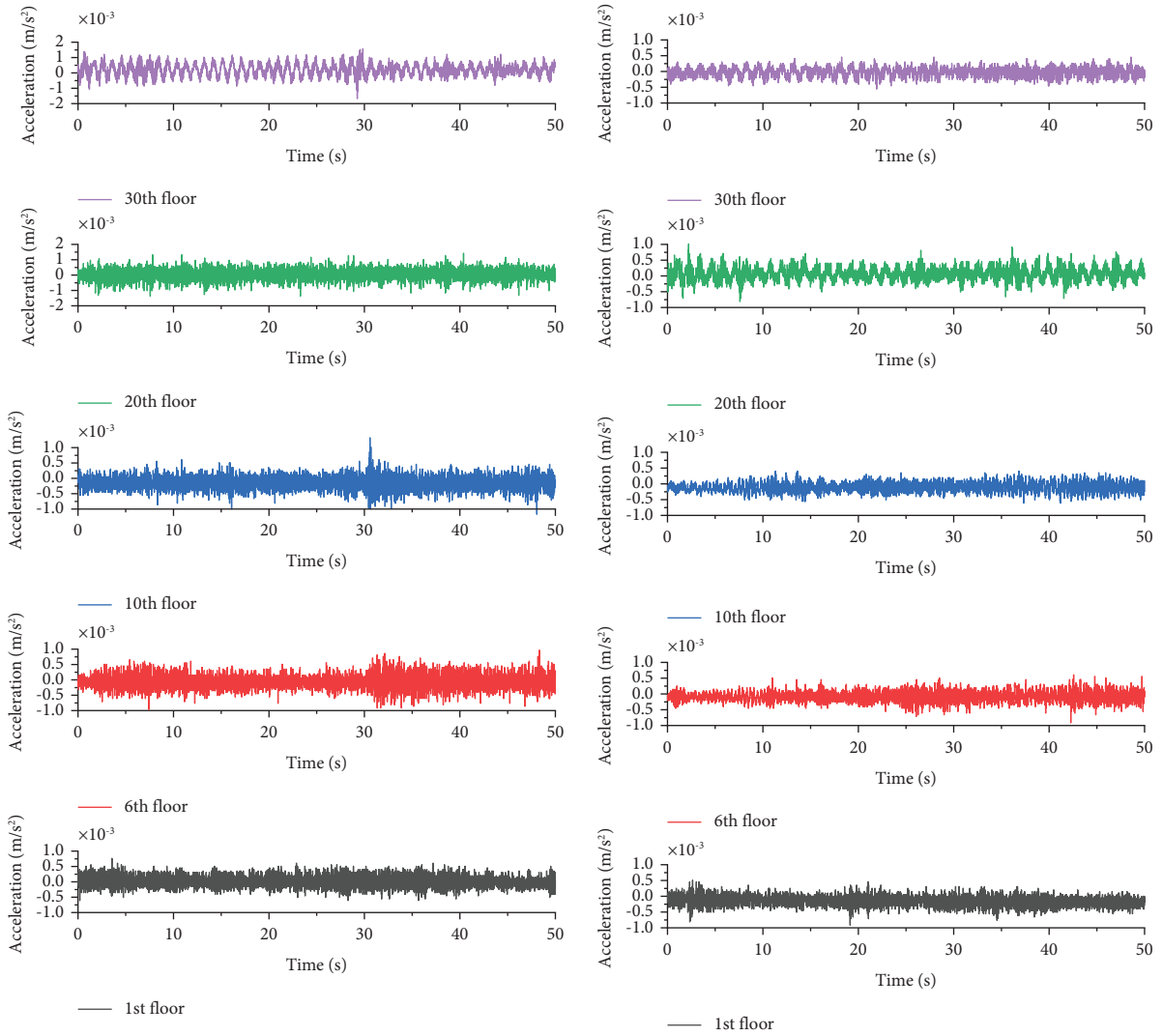


FIGURE 12: The time history of acceleration: (a) the X direction and (b) the Y direction.

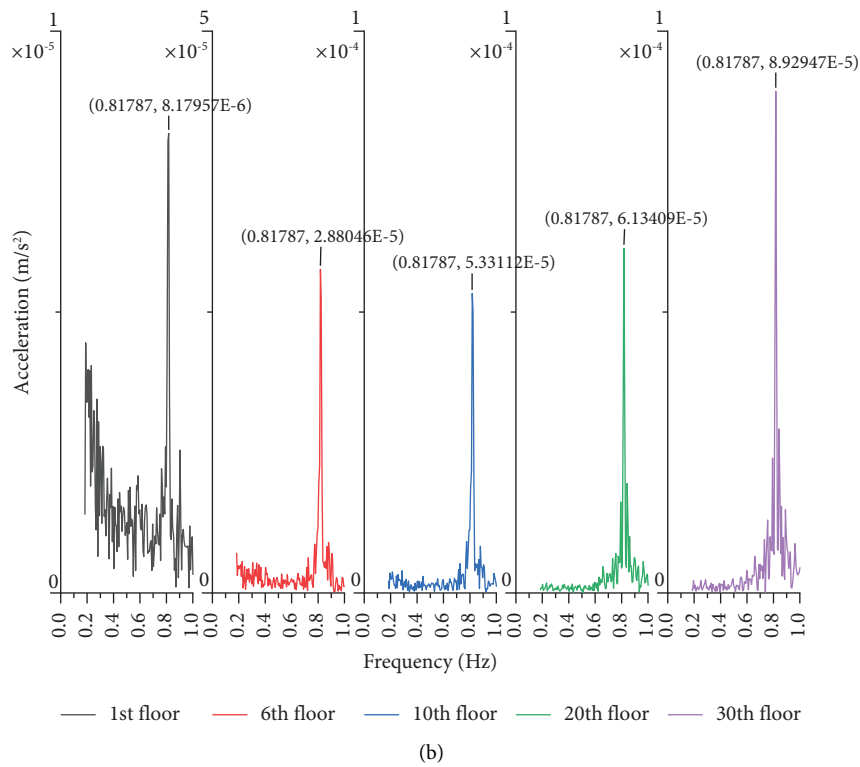
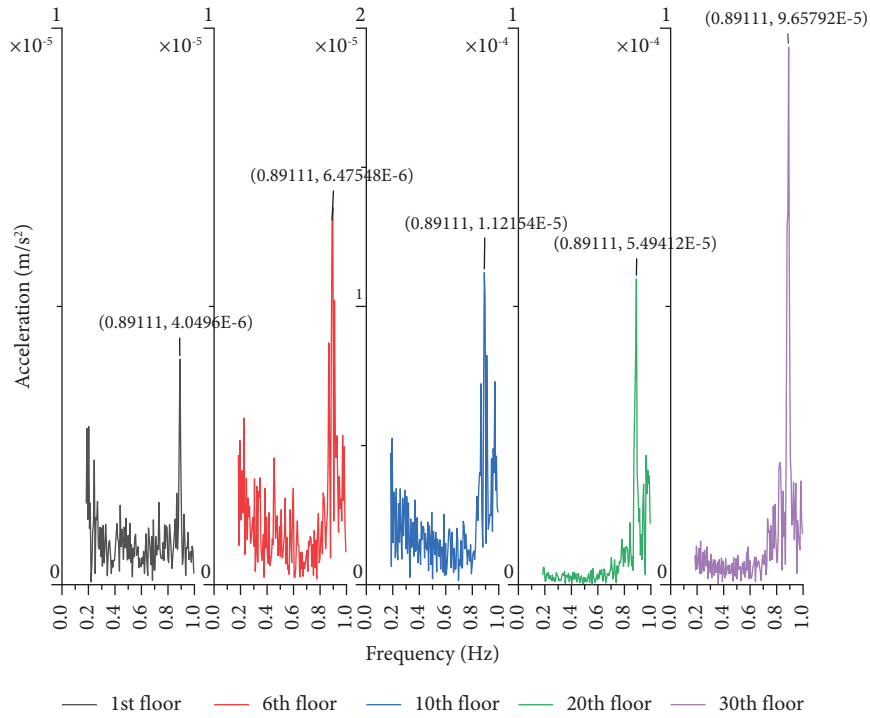


FIGURE 13: The spectra of acceleration: (a) the X direction and (b) the Y direction.

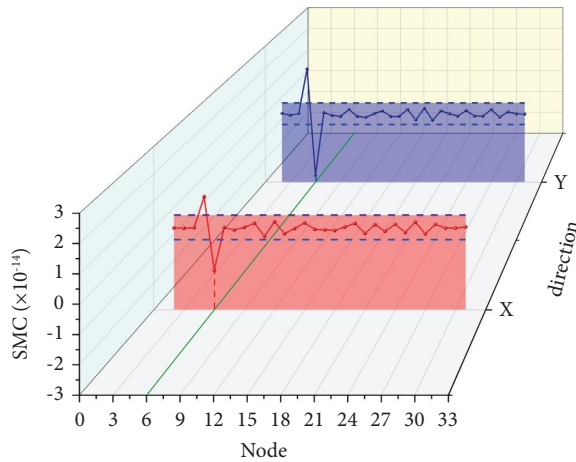


FIGURE 14: Identification result of the high-rise building.

5. Conclusions

This paper introduces a baseline-free method for detecting abrupt changes in lateral stiffness of high-rise buildings using SMC. The method eliminates the need for a baseline, making it highly practical. The approach's validity is substantiated through a combination of numerical simulations and field test investigations. The ensuing conclusions are delineated as follows:

- (1) The measured displacement response is used to compute the second-order SMC of relative displacement. Utilizing the box plot technique, upper and lower limits are established to discern abrupt shifts in the curve. This information is subsequently used to identify the location of the abrupt lateral stiffness change.
- (2) This method is applicable to constant stiffness, gradual stiffness, and stiffness stage-changing structures and has a good identification result with various external excitations and different levels of environmental noise.
- (3) This method does not need the prior information of the structure, and it can evaluate the state of the structure only according to measurement. At the same time, SMC is a time-domain index, which is easy to obtain and simple to calculate. It is especially suitable for the on-site rapid preliminary detection of high-rise building structures after earthquakes and other disasters.

Data Availability

The data that support the findings of this study are available from the corresponding author upon reasonable request.

Conflicts of Interest

The authors declare that they have no conflicts of interest.

Acknowledgments

We are grateful to the following agencies for their supports in this study: Innovation Group Project of the National Natural Science Foundation of China (Grant no. 52221002), Graduate Research and Innovation Foundation of Chongqing, China (Grant nos. CYS22053 and CYS22049), and Chongqing High-Tech Zone Science and Technology Innovation Bureau Project: Research on key technologies of prefabricated, intelligent construction and intelligent operation, and maintenance under EPC mode.

References

- [1] X. M. Lei, L. M. Sun, and Y. Xia, "Lost data reconstruction for structural health monitoring using deep convolutional generative adversarial networks," *Structural Health Monitoring*, vol. 20, no. 4, pp. 2069–2087, 2021.
- [2] Y. Xia, X. M. Lei, P. Wang, G. M. Liu, and L. M. Sun, "Long-term performance monitoring and assessment of concrete beam bridges using neutral axis indicator," *Structural Control and Health Monitoring*, vol. 27, no. 12, 2020.
- [3] Y. Yang, W. Xu, Z. Gao, Z. Yu, and Y. Zhang, "Research progress of SHM system for super high-rise buildings based on wireless sensor network and cloud platform," *Remote Sensing*, vol. 15, no. 6, p. 1473, 2023.
- [4] Y. Yang, H. Lu, X. Tan, H. K. Chai, R. Wang, and Y. Zhang, "Fundamental mode shape estimation and element stiffness evaluation of girder bridges by using passing tractor-trailers," *Mechanical Systems and Signal Processing*, vol. 169, Article ID 108746, 2022.
- [5] Y. Yang, H. Lu, X. Tan, R. Wang, and Y. Zhang, "Mode shape identification and damage detection of bridge by movable sensory system," *IEEE Transactions on Intelligent Transportation Systems*, vol. 24, no. 1, pp. 1299–1313, 2023.
- [6] P. Cawley and R. D. Adams, "The location of defects in structures from measurements of natural frequencies," *The Journal of Strain Analysis for Engineering Design*, vol. 14, no. 2, pp. 49–57, 1979.
- [7] D. F. Mazurek and J. T. Dewolf, "Experimental study of bridge monitoring technique," *Journal of Structural Engineering*, vol. 116, no. 9, pp. 2532–2549, 1990.
- [8] K. M. Liew and Q. Wang, "Application of wavelet theory for crack identification in structures," *Journal of Engineering Mechanics*, vol. 124, no. 2, pp. 152–157, 1998.
- [9] Y. Y. Lee and K. M. Liew, "Detection of damage locations in a beam using the wavelet analysis," *International Journal of Structural Stability and Dynamics*, vol. 1, no. 3, pp. 455–465, 2001.
- [10] I. Mekjavi and D. Damjanovi, "Damage assessment in bridges based on measured natural frequencies," *International Journal of Structural Stability and Dynamics*, vol. 17, Article ID 1750022, 2016.
- [11] W. M. West, *Illustration of the Use of Modal Assurance Criterion to Detect Structural Changes in an Orbiter Test Specimen*, NASA Johnson Space Center, Houston, TX, USA, 1986.
- [12] Z. Y. Shi, S. S. Law, and L. M. Zhang, "Damage localization by directly using incomplete mode shapes," *Journal of Engineering Mechanics*, vol. 126, no. 6, pp. 656–660, 2000.

- [13] V. Shahsavari, L. Chouinard, and J. Bastien, "Wavelet-based analysis of mode shapes for statistical detection and localization of damage in beams using likelihood ratio test," *Engineering Structures*, vol. 132, pp. 494–507, 2017.
- [14] H. P. Zhu, L. Li, and X. Q. He, "Damage detection method for shear buildings using the changes in the first mode shape slopes," *Computers and Structures*, vol. 89, no. 9-10, pp. 733–743, 2011.
- [15] D. Dessi and G. Camerlengo, "Damage identification techniques via modal curvature analysis: overview and comparison," *Mechanical Systems and Signal Processing*, vol. 52-53, pp. 181–205, 2015.
- [16] S. M. H. Pooya and A. Massumi, "A novel and efficient method for damage detection in beam-like structures solely based on damaged structure data and using mode shape curvature estimation," *Applied Mathematical Modelling*, vol. 91, pp. 670–694, 2021.
- [17] M. Cao, M. Radzienski, W. Xu, and W. Ostachowicz, "Identification of multiple damage in beams based on robust curvature mode shapes," *Mechanical Systems and Signal Processing*, vol. 46, no. 2, pp. 468–480, 2014.
- [18] M. Cao, W. Xu, W. Ostachowicz, and Z. Su, "Damage identification for beams in noisy conditions based on Teager energy operator-wavelet transform modal curvature," *Journal of Sound and Vibration*, vol. 333, no. 6, pp. 1543–1553, 2014.
- [19] M. He, T. Yang, and Y. Du, "Nondestructive identification of composite beams damage based on the curvature mode difference," *Composite Structures*, vol. 176, pp. 178–186, 2017.
- [20] Z. B. Yang, M. Radzienski, P. Kudela, and W. Ostachowicz, "Fourier spectral-based modal curvature analysis and its application to damage detection in beams," *Mechanical Systems and Signal Processing*, vol. 84, pp. 763–781, 2017.
- [21] J. Y. Shi, B. F. Spencer, and S. S. Chen, "Damage detection in shear buildings using different estimated curvature," *Structural Control and Health Monitoring*, vol. 25, no. 1, 2018.
- [22] H. Cao and M. I. Friswell, "Nondestructive damage evaluation indicator based on modal flexibility curvature," *Engineering Mechanics*, vol. 23, pp. 33–38, 2006.
- [23] H. Cao, X. L. Zhang, and Y. M. Li, "Damage evaluation of frames by modal flexibility curvature," *Journal of Vibration and Shock*, vol. 26, pp. 116–117, 2007.
- [24] D. Dinh-Cong, T. Nguyen-Thoi, and D. T. Nguyen, "A two-stage multi-damage detection approach for compo-site structures using MKECR-Tikhonov regularization iterative method and model updating procedure," *Applied Mathematical Modelling*, vol. 90, pp. 114–130, 2021.
- [25] D. Dinh-Cong, T. T. Truong, and T. Nguyen-Thoi, "A comparative study of different dynamic condensation techniques applied to multi-damage identification of FGM and FG-CNTRC plates," *Engineering with Computers*, vol. 38, no. S5, pp. 3951–3975, 2021.
- [26] J. Zhang, Y. L. Xu, Y. Xia, and J. Li, "A new statistical moment-based structural damage detection method," *Structural Engineering and Mechanics*, vol. 30, no. 4, pp. 445–466, 2008.
- [27] D. S. Wang, W. Xiang, and H. P. Zhu, "Damage identification in beam type structures based on statistical moment using a two step method," *Journal of Sound and Vibration*, vol. 333, no. 3, pp. 745–760, 2014.
- [28] Y. Yang, J. L. Li, C. H. Zhou, S. S. Law, and L. Lv, "Damage detection of structures with parametric uncertainties based on fusion of statistical moments," *Journal of Sound and Vibration*, vol. 442, pp. 200–219, 2019.
- [29] Y. Yang, Y. Ling, X. K. Tan, S. Wang, and R. Q. Wang, "Damage identification of frame structure based on approximate Metropolis-Hastings algorithm and probability density evolution method," *International Journal of Structural Stability and Dynamics*, vol. 22, no. 03n04, Article ID 2240014, 2022.
- [30] D. Dinh-Cong, T. Pham-Toan, D. Nguyen-Thai, and T. Nguyen-Thoi, "Structural damage assessment with incomplete and noisy modal data using model reduction technique and LAPO algorithm," *Structure and Infrastructure Engineering*, vol. 15, no. 11, pp. 1436–1449, 2019.
- [31] C. J. Chang, D. C. Li, Y. H. Huang, and C. C. Chen, "A novel gray forecasting model based on the box plot for small manufacturing data sets," *Applied Mathematics and Computation*, vol. 265, pp. 400–408, 2015.
- [32] P. Khemmoook, S. Khomfoi, T. Phophongviwat, and W. Pairindra, "Deteriorated solar panel detection technique of SST for a solar farm application," in *Proceedings of the 2019 7th International Electrical Engineering Congress (iEECON)*, Hua Hin, Thailand, March 2019.
- [33] J. Zhao and J. T. Dewolf, "Sensitivity study for vibrational parameters used in damage detection," *Journal of Structural Engineering*, vol. 125, no. 4, pp. 410–416, 1999.